

Supporting Information

Highly Sensitive CWA Sensing Materials Based on Tetrafluorophenol Modified s-SWCNTs

Jenner H. L. Ngai,¹ Zhao Li,¹ Shiliang Wang,² Oltion Kodra,³ François Lapointe,¹ Patrick R. L. Malenfant¹ and Jianfu Ding*¹

¹Quantum and Nanotechnologies Research Centre and ³Clean Energy Innovation Research Centre, National Research Council Canada, 1200 Montreal Road, Ottawa, Ontario, K1A 0R6, Canada; ²Suffield Research Centre, Defense Research and Development Canada, PO Box 4000, Station Main, Medicine Hat, Alberta, T1A 8K6, Canada.

holoongjenner.ngai@nrc-cnrc.gc.ca; zhao.li@nrc-cnrc.gc.ca; shiliang.wang@forces.gc.ca; oltion.kodra@nrc-cnrc.gc.ca; francois.lapointe@nrc-cnrc.gc.ca. patrick.malenfant@nrc-cnrc.gc.ca. *Correspondence: jianfu.ding@nrc-cnrc.gc.ca.

1. Set-up for DMMP sensor test.

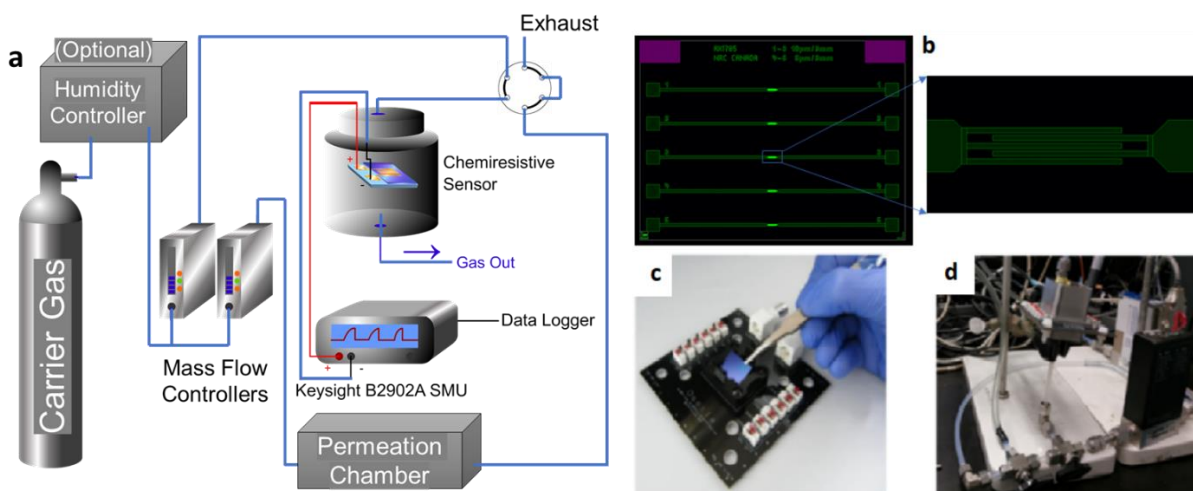


Figure S1. (a) Set-up of the DMMP sensing system, where the flow rate of DMMP gas and carrier gas was kept constant, while the temperature in permeation chamber is controlled at different values to achieve different DMMP gas concentrations in the testing chamber. (b) Photos of the Ossila chip. (c) A photo of the Ossila chip holder isolated from the testing chamber. (d) A photo of the testing chamber (the metal cube in the top center).

2. UV-vis-NIR absorption spectra the SWCNTs before and after TFP functionalization.

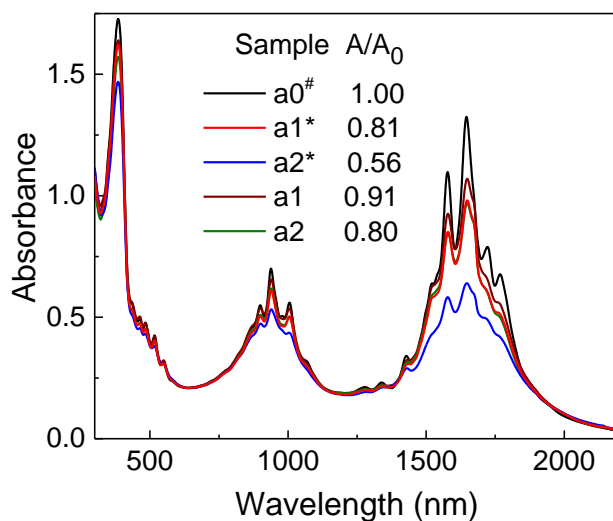


Figure S2. UV-vis-NIR absorption spectra of the redispersed solution in toluene of TFP-SWCNTs products from the reaction in DMAc (a1* and a1) and *o*DCB (a2* and a2). The asterisk (*) denotes samples before TEA treatment. Spectrum of the pristine SWCNTs (a0[#]) is included for comparison.

3. FT-IR characterization of PFDD before and after the reaction with ATFP.

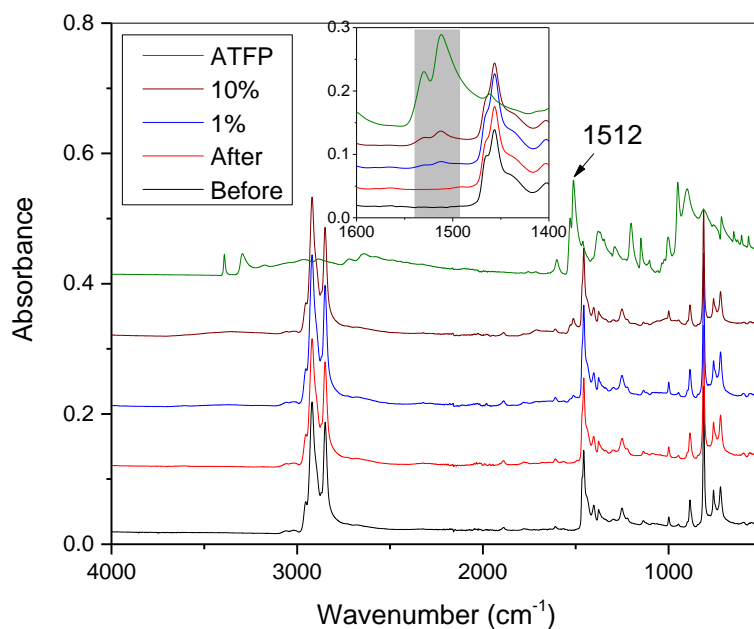


Figure S3, ART-FTIR spectra of PFDD before and after reacting with ATFP at the same conditions as for preparing sample a1, and compared with the spectra of ATFP/PFDD mixtures at 1 % and 10 % ATFP contents, and pure ATFP crystal.

4. Characterization data of the b-series samples.

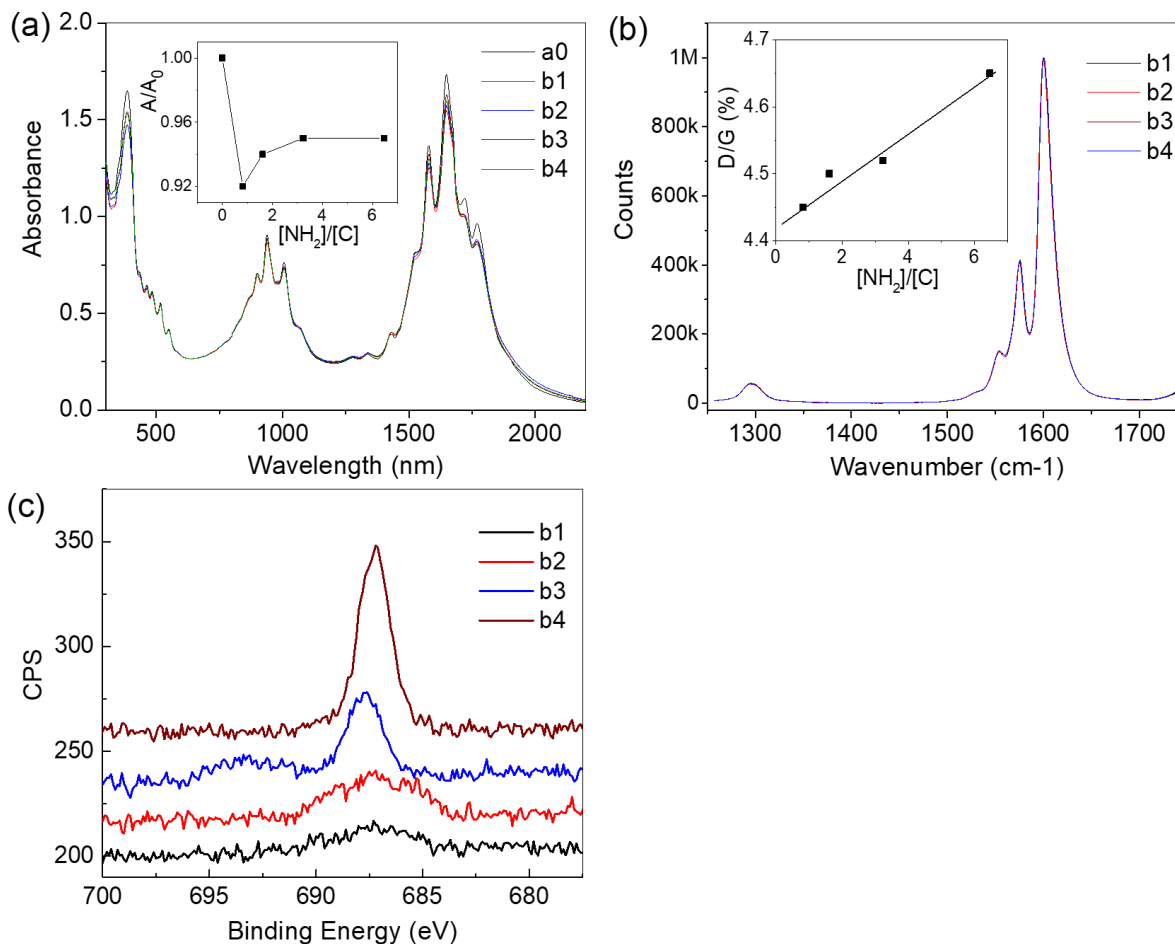


Figure S4. Characterization data of the b-series samples from the reactions in DMAc for 4 h at the $[NH_2]/[C]$ feed ratio of 0.81 (b1), 1.61 (b2), 3.23 (b3) and 6.46 (b4): (a) UV spectra and the variation of A/A_0 with $[NH_2]/[C]$ ratio (inset); (b) D and G band of Raman spectrum of the samples on a PTFE filter membrane excited by 785 nm laser, and the variation of D/G (%) with $[NH_2]/[C]$ ratio (inset); and (c) F 1s curve of the XPS spectra normalized to the C 1s band.

5. DMMP sensing profiles of devices b1, b4, c4, d1 and d2 tested in dry air.

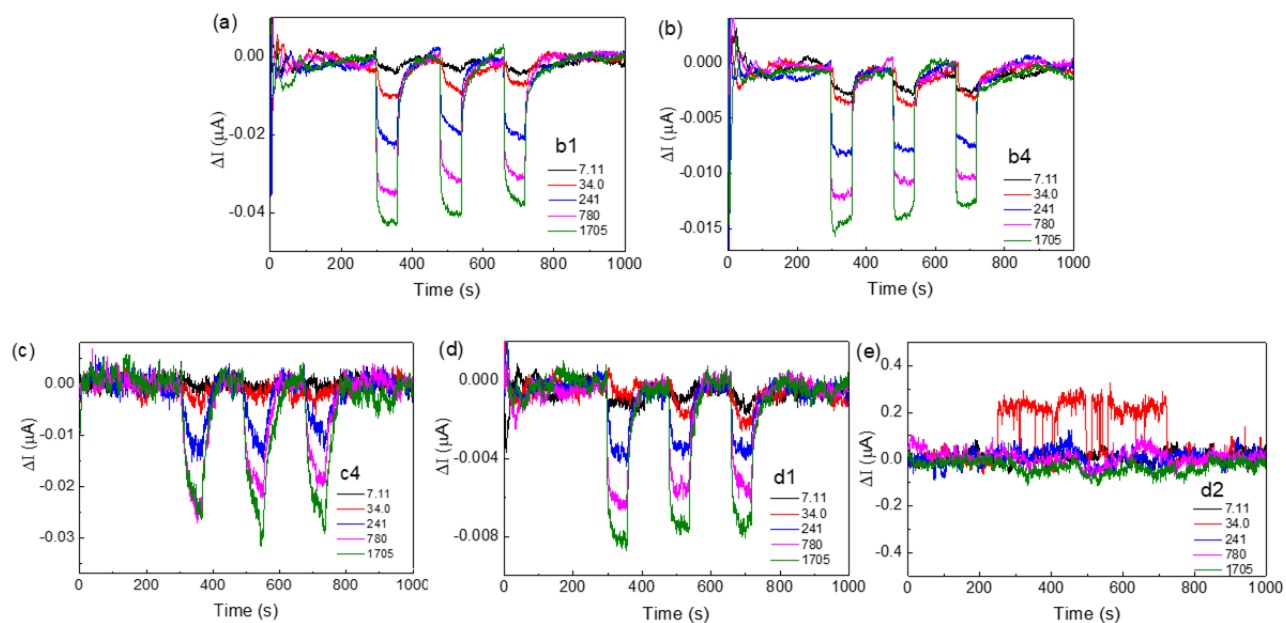


Figure S5. Dynamic DMMP sensing profiles of TFP-SWCNTs devices tested in dry air for (a) sample b1, (b) sample b4, (c) sample c4, (d) samples d1 and (e) sample d2. The reaction conditions for the preparation of each sample can be seen in the caption of Figure 4.

6. DMMP sensing profiles of devices b1, b4, c4, d1 and d2 tested in humid air at 15% RH.

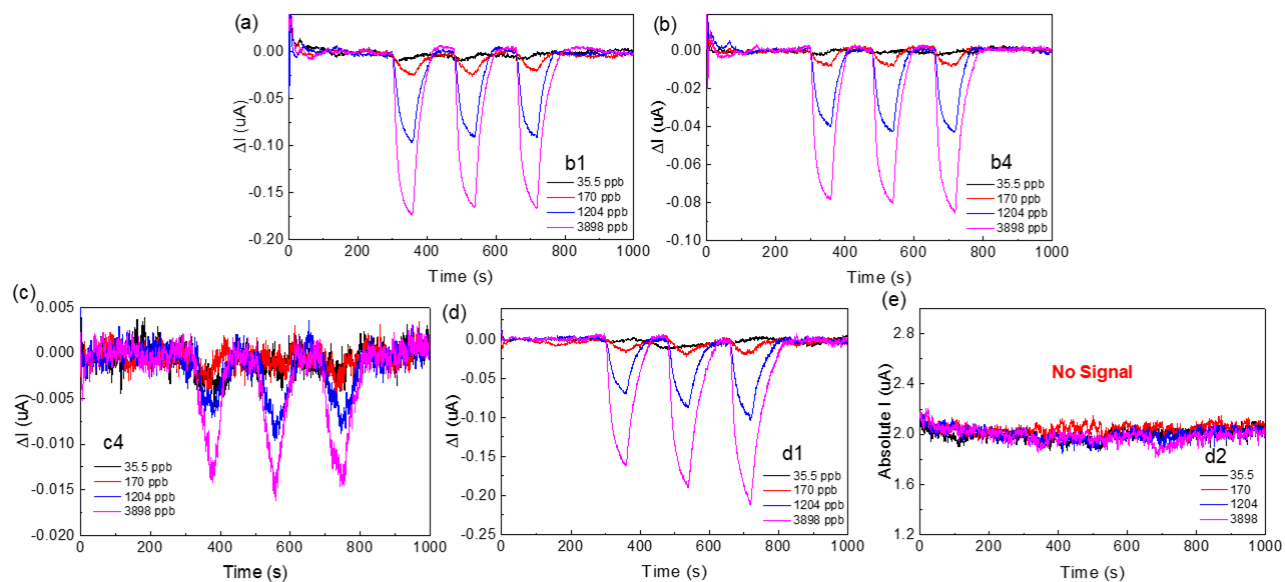


Figure S6. Dynamic DMMP sensing profiles of TFP-SWCNTs samples tested in humid air at 15% RH for (a) sample b1, (b) sample b4, (c) sample c4, (d) samples d1 and (e) sample d2. The reaction conditions for the preparation of each sample can be seen in the caption of Figure 4.

7. Power spectra density of devices b1, b4, d1 and d2 in different carrier gas.

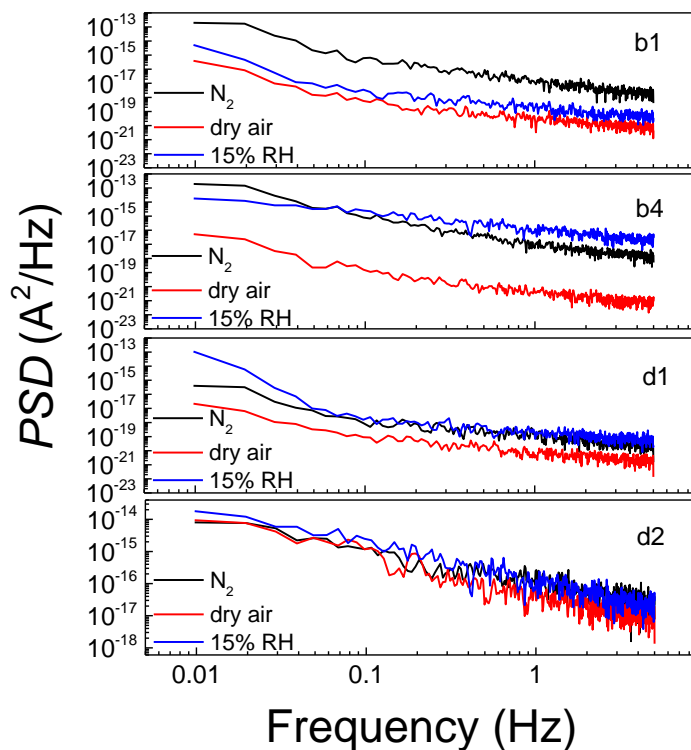


Figure S7. Power spectra density (PSD) of the samples b1, b4, d1 and d2 before DMMP gas introduction in different carrier gases. PSD represents the overall noise level characteristics in the test conditions.

8. Computer simulated Gibbs free energy level of *Models 1, 2, 3, and 4*.

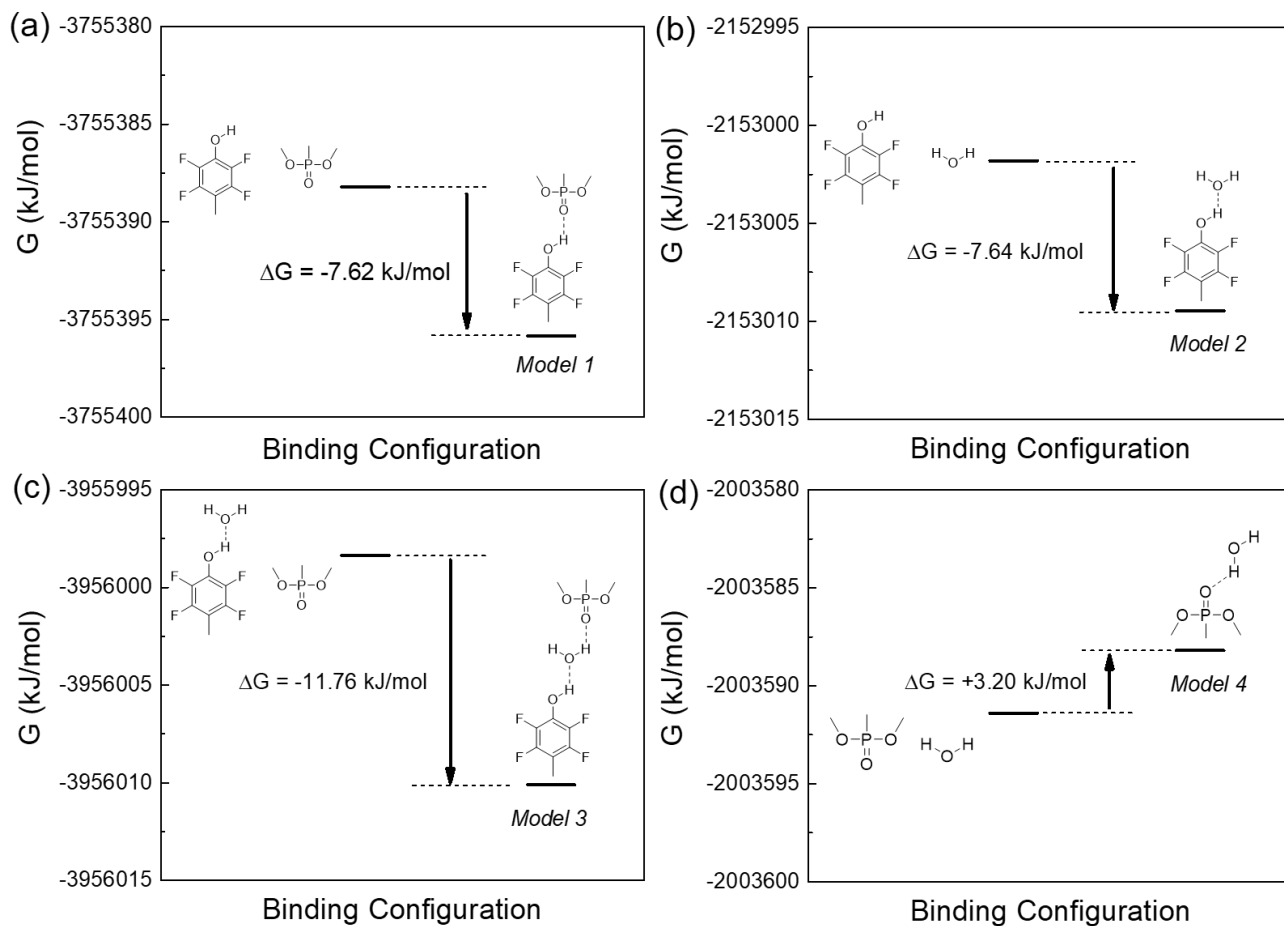


Figure S8. Computer simulated Gibbs free energy level with respect to complex formation processes. Change in energy levels represented complex formation energy and spontaneity of the four simulation complex models (a) *Model 1*; (b) *Model 2*; (c) *Model 3*; and (d) *Model 4*.

9. VOC sensing tests of selected TFP-SWCNTs samples (b1, b4 and d1).

Table S1 General Details of VOC Permeation Tubes.

Permeation Tube	Permeation Rate (ng/min)	MW (g/mol)	Ref Temperature (°C)	Lowest conc (ppb)
DMMP	4327.4	124.08	100	7.11 @ 500sccm
Methanol	982.96	32.04	30	1500 @ 500sccm
Acetone	2089.66	58.08	40	804 @ 500sccm
Toluene	2866.19	92.141	50	318 @ 500sccm
DMF	1413.53	73.09	60	90 @ 500sccm

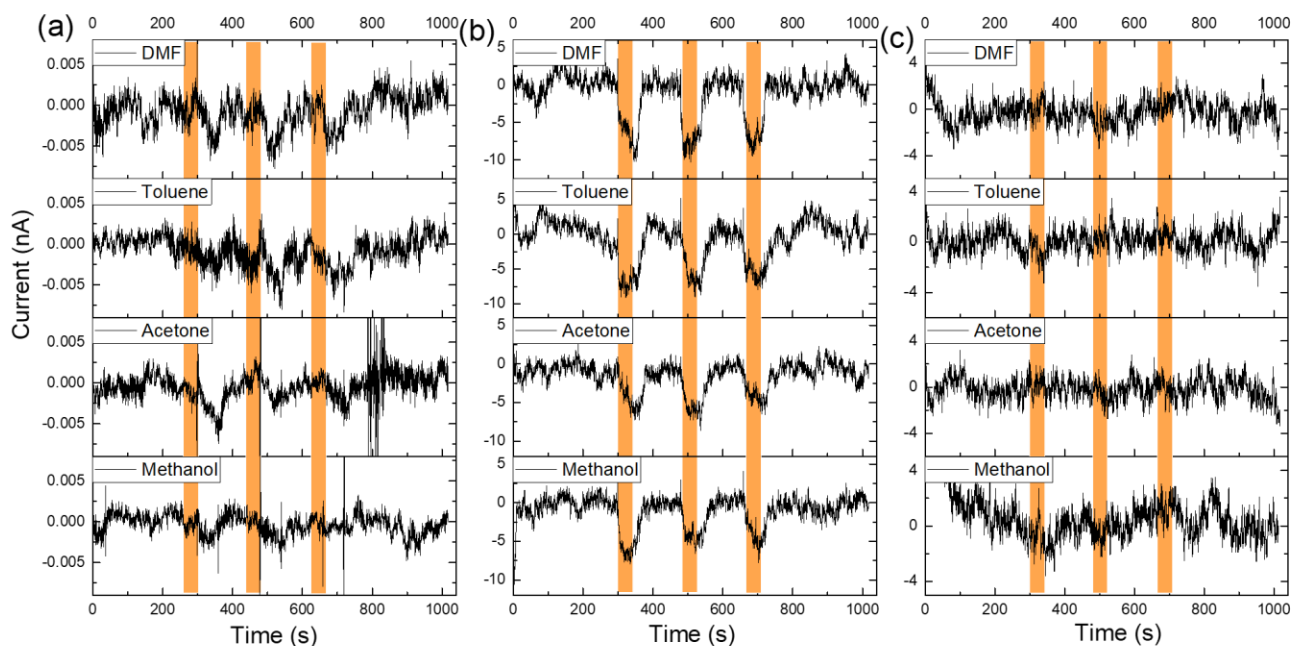


Figure S9. Dynamic sensing response of devices in dry N_2 for (a) sample b1; (b) sample b4; and (c) sample d1 towards different VOC gases including methanol, acetone, toluene, and *N-N'*-dimethylformamide (DMF) at the lowest concentration listed in Table S1. Each graph displays the response to three successive VOC gas injections shown as red shaded areas.

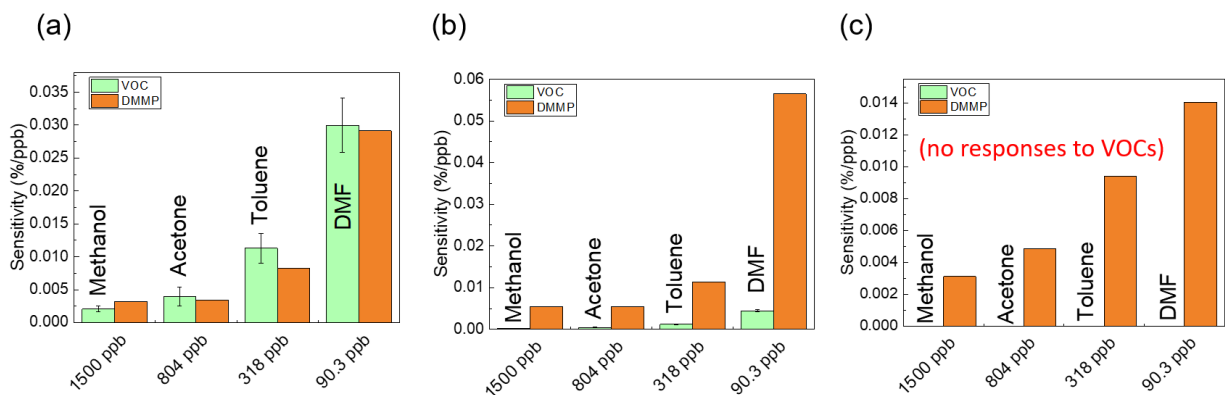


Figure S10. Comparison of concentration-normalized sensitivities for various VOCs and DMMP for (a) sample b1; (b) sample b4 and (c) sample d1. The DMMP sensitivities at specific concentrations corresponding to those of the tested VOCs were derived from the calibration curves from Figure 5a.